Dyes and Pigments 88 (2011) 65–74

Contents lists available at ScienceDirect

Dyes and Pigments

journal homepage: www.elsevier.com/locate/dyepig

The synthesis and characterisation of carbohydrate-functionalised porphyrazines

D. Bradley G. Williams*, G. Bheki Mbatha

Department of Chemistry, University of Johannesburg, P.O. Box 524, Auckland Park 2006, Johannesburg, South Africa

ARTICLE INFO

Article history:
Received 25 March 2010
Received in revised form
7 May 2010
Accepted 10 May 2010
Available online 19 May 2010

Keywords:
Porphyrazine
Carbohydrate
Macrocycle
Photodynamic therapy
Extraction coefficient
Chiral

ABSTRACT

A synthetic pathway to the incorporation of mono- and disaccharide carbohydrate moieties into porphyrazine systems was demonstrated. A range of selectively protected monosaccharide precursors was coupled to a small variety of phthalonitriles; the intermediates were co-macrocyclised to form hybrid porphyrazines in Linstead macrocyclisation reactions. Demetallisation of Mg-porphyrazine products was readily effected to afford the free-base pigments, which were subsequently converted into their zinc or nickel complexes. Some porphyrazines were deprotected of their isopropylidene groups (on the carbohydrate moieties) under acidic conditions to reveal polar OH groups. The extraction coefficients of the porphyrazines between 2-octanol and phosphate buffered saline solution were measured. Comparison of the partition coefficients of the carbohydrate-substituted porphyrazines and their deprotected counterparts revealed that structural alteration offers a way to significantly increase the hydrophilicity of substituted porphyrazines.

1. Introduction

The synthesis, properties and application of porphyrazines have received increasing attention in recent years [1–3], especially their potential role as photosensitisers in photodynamic therapy [4–8]. A continuing problem in photodynamic therapy is selectivity of uptake of the photosensitiser by cancerous tissue, for which a potential solution, is functionalisation of the photosensitiser with a biological moiety (e.g. a carbohydrate) to assist its selective uptake and improve its solubility. Substituted amphiphilic and hydrophilic porphyrazines bearing both hydrophilic and hydrophobic moieties have been shown to be potent photosensitisers in photodynamic therapy [9–12]. Such pigments should be sufficiently hydrophilic to be administered as aqueous solutions so as to ensure that they quickly reach the target tumour tissues once administered and are rapidly eliminated from the body post clinic.

Carbohydrates play a central role in various biological recognition processes with many carbohydrate-derived therapeutics undergoing clinical trials [13–16]. The idea of employing saccharides as conjugates to manipulate drug distribution is also of interest and has been used to good effect in other instances [17,18]. Additionally, deprotection of carbohydrate-substituted compounds brings another advantage by increasing the solubility of the molecules in aqueous media, a phenomenon which would be of more general interest than exclusively in the medical application of these macrocycles. In this paper, we report the synthesis of porphyrazines with carbohydrate substituents, on metal complexation (in the cavity) thereof and the removal of the isopropylidene protecting groups seated on the carbohydrate residues. We also report on the influence on the hydrophilicity of the porphyrazine ring system with structural alteration of the carbohydrate moieties as measured against pigments **1** and **2** (Fig. 1).

2. Experimental

Under this section, only representative examples are given. Full details for the preparation and analyses of all new compounds are given under Supplementary Information (for compounds 6, 7, 10–12, 18, 21, 23, 25, 26, 28, 29, 35, 37–39, 41–43, 45–48, 50–66, 63–65). Copies of selected UV–vis spectra are also reproduced.

All solvents used were purified according to the purification of laboratory chemicals and the reactions were done under nitrogen atmosphere [19]. Flash column chromatography was carried out on Merck Kieselgel 60 (230–400 mesh) under nitrogen pressure. Thin-layer chromatography was performed using Merck 60 F_{254} silica gel sheets. NMR spectra were recorded on a Varian Gemini 300 MHz spectrometer in $CDCl_3$ or DMSO unless otherwise indicated. Electronic spectra were measured on a UV–visible160 An SHIMADZU spectrophotometer, using a matched pair of 1 cm path length quartz cuvettes. Melting points were determined on a REICHERT Koffler hot stage melting point apparatus and are uncorrected. The phosphate buffered saline solution was prepared by dissolving the

* Corresponding author. Tel.: +27 115593431; fax: +27 11 559 2819.
E-mail address: bwilliams@uj.ac.za (D.B.G. Williams).

0143-7208/$ – see front matter © 2010 Elsevier Ltd. All rights reserved.
doi:10.1016/j.dyepig.2010.05.002

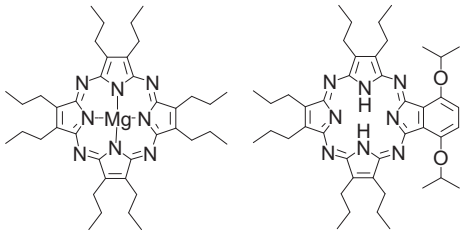

Fig. 1. Porphyrazines used for comparison purposes.

tablets (Fluka) in purified water (Burdick and Jackson or Fluka), followed by boiling the solution for 5–15 min and cooling to room temperature. PBS solutions were used within seven days.

Dichlorophthalonitrile **14**, octapropylporphyrazine **1**, *trans*-porphyrazine **2**, 3-nitrophthalonitrile **17** and 2,3-dipropylmaleonitrile **30**, were prepared according to published procedures [20–22].

2.1. Synthesis

2.1.1. Galactosyl/galactosyl disaccharide **8**

Pyranose **7** (800 mg, 1.24 mmol) was dissolved in methanol (20 mL), to which was then added 10% Pd/C (80 mg) and the suspension pressurised with hydrogen gas at 350 kPa for 12 h. The catalyst was filtered off and the product was chromatographed (hexane/ethyl acetate, 1:1) to give **8** (623 mg, 1.12 mmol, 90%). R_f 0.47 (hexane/ethyl acetate, 1:1); ^{1}H NMR (300 MHz, $CDCl_3$) δ_H: 5.42 (1H, d, $J = 4.5$ Hz), 4.86 (3H, m), 4.67 (6H, br s), 4.90 (1H, t, $J = 7.8$ Hz), 4.27 (1H, d, $J = 7.8$ Hz), 4.18 (1H, m), 3.96 (1H, m), 3.90 (1H, s br, OH), 3.60 (4H, m), 3.47 (1H, t, $J = 6.6$ Hz), 3.34 (6H, s br), 3.33 (3H, s), 1.40 (3H, s), 1.30 (3H, s), 1.23 (6H, s); ^{13}C NMR (75 MHz, $CDCl_3$) δ_C: 109.2, 108.9, 103.9, 98.0, 97.3, 96.4, 96.2, 74.9, 74.1, 73.2, 71.2, 70.6, 70.3, 69.4, 67.3, 60.8, 60.2, 55.9, 55.7, 55.6, 25.8 (2C), 24.8, 24.2; FAB-MS: 555 ($[M]^+$); IR υ_{max} ($CHCl_3$)/cm^{-1}: 3249, 2867, 2801, 1367, 1231.

2.1.2. Ribosyl/galactosyl disaccharide **13**

The reaction was performed according to that recounted for **8** above. Yield (805 mg, 1.62 mmol, 73%); R_f 0.61 (hexane/acetone, 1:1); ^{1}H NMR (300 MHz, $CDCl_3$) δ_H: 4.88 (1H, s), 4.83 (2H, m), 4.70 (6H, br s), 4.50 (1H, t, $J = 5.7$ Hz), 4.28 (2H, m), 3.93 (1H, br s), 3.75 (3H, m), 3.53 (4H, m), 3.74 (6H, s), 3.36 (3H, s), 3.20 (3H, s), 1.41 (3H, s), 1.25 (3H, s); ^{13}C NMR (75 MHz, $CDCl_3$) δ_C: 112. 3, 109.1, 103.8, 98.0, 97.5, 96.5, 85.2, 84.9, 82.1, 75.3, 74.5, 73.2, 71.1, 61.0, 56.2, 56.0, 55.8, 54.8, 25.3, 24.8; FAB-MS: 497 ($[M - 1]^+$), 467 ($[M-OCH_3]^+$); IR υ_{max} ($CHCl_3$)/cm^{-1}: 3466, 3019, 2994, 2933, 1339, 1208.

2.1.3. Ribose-substituted phthalonitrile **15**

A stirred solution of 4,5-dichlorophthalonitrile (1.60 g, 8.00 mmol) and 1-*O*-methyl-2,3-*O*-methylidene-D-(−)-ribose **9** (4.30 g, 21.0 mmol) in dry DMSO (20 mL) was heated to 90 °C. To the ensuing mixture was added dry, finely powdered potassium carbonate (3.50 g, 25.0 mmol) in four equal portions over 30 min. The mixture was stirred at 90 °C for 3 h after which it was poured into ice-cold water. The precipitate formed was filtered, washed with water and re-dissolved in ethyl acetate. Evaporation of the solvent followed by flash silica chromatography (hexane/ethyl acetate, 1:2) gave compound **15** which was re-crystallised from methanol (1.17 g, 3.20 mmol, 40%). R_f 0.51 (ethyl acetate/hexane, 1:2); mp 189–192 °C; $[\alpha]_D$ −38.3° (*c* 0.196, $CHCl_3$); ^{1}H NMR (300 MHz, $CDCl_3$) δ_H: 7.84 (1H, s), 7.31 (1H, s), 5.08 (1H, s), 4.84 (1H, d, $J = 6.2$ Hz), 4.70 (1H, d, $J = 6.2$ Hz), 4.65 (1H, t, $J = 6.2$ Hz), 4.19 (2H, m), 3.40 (3H, s), 1.56 (3H, s), 1.39 (3H, s); ^{13}C NMR (75 MHz, $CDCl_3$) δ_C: 157.3, 134.8, 129.1, 116.7, 115.5, 114.7, 114.4, 112.8, 109.7, 108.7, 84.9, 83.6, 81.7, 70.2, 55.4, 26.4, 25.0; FAB-MS: 367 ($[M + 1]^+$), 333 ($[M-OCH_3-2H]^+$), 307 ($[M-OCH_3-C_2H_4]^+$); IR υ_{max} ($CHCl_3$)/cm^{-1}: 3082, 2998, 2230, 1317, 1225, 1053, 703.

2.1.4. Phenoxy-substituted phthalonitrile **16**

The reaction was performed according to the synthesis of **15** described above, using phenol as the second nucleophile. White crystals, yield (0.62 g, 2.0 mmol, 67%); R_f 0.26 (ethyl acetate/hexane, 1:2); mp 130–135 °C; $[\alpha]_D$ −40.9° (*c* 0.164, $CHCl_3$); ^{1}H NMR (300 MHz, $CDCl_3$) δ_H: 7.44 (2H, t, $J = 7.3$ Hz), 7.30 (1H, s), 7.27 (1H, d, $J = 7.3$ Hz), 7.13 (1H, s), 6.98 (2H, d, $J = 7.3$ Hz), 4.96 (1H, s), 4.63 (1H, d, $J = 5.9$ Hz), 4.60 (1H, d, $J = 5.9$ Hz), 4.52 (1H, t, $J = 7.1$ Hz), 4.14 (2H, m), 3.35 (3H, s), 1.50 (3H, s), 1.27 (3H, s); ^{13}C NMR (75 MHz, $CDCl_3$) δ_C: 154.5, 152.4, 151.0, 130.4 (2C), 125.5, 121.8, 119.5 (2C), 117.8, 115.3, 115.1, 112.7, 110.7, 109.7, 109.1, 84.9, 83.6, 81.7, 69.9, 55.3, 26.4, 25,0; FAB-MS: 422 ($[M]^+$), 407 ($[M - CH_3]^+$), 391 ($[M-OCH_3]^+$); IR υ_{max} ($CHCl_3$)/cm^{-1}: 3051, 2979, 2945, 2937, 2231, 1367, 1199, 1006.

2.1.5. Ribose-derived phthalonitrile **19**

General route for the coupling of carbohydrates to nitrophthalonitriles in the presence of NaH as the base: A solution of 1-*O*-methyl-2,3-*O*-methylidene-D-ribose (1.20 g, 5.88 mmol) in DMF (45 mL) was added to 60% NaH (306 mg, 7.64 mmol) at 0 °C. The reaction mixture was stirred at 0 °C for 30 min after which 3-nitrophthalonitrile (1.22 g, 7.06 mmol) was added and then stirred at room temperature for 5 days. The ensuing mixture was poured into ethyl acetate (600 mL) and washed with water (100 mL × 3). The organic layer was dried with $MgSO_4$. After evaporation of the solvent, the product was purified by flash column chromatography (ethyl acetate) to yield **19** as white crystals from ethyl acetate (637 mg, 1.93 mmol, 33%). R_f 0.31 (ethyl acetate); mp 162–167 °C; $[\alpha]_D$ −54.6° (*c* 0.218, $CHCl_3$); ^{1}H NMR (300 MHz, $CDCl_3$) δ_H: 7.57 (1H, t, $J = 7.6$ Hz), 7.44 (1H, d, $J = 7.6$ Hz), 7.11 (1H, d, $J = 7.6$ Hz), 5.06 (1H, s), 4.80 (1H, d, $J = 6.0$ Hz), 4.67 (1H, d, $J = 6.0$ Hz), 4.61 (1H, t, $J = 6.3$ Hz), 4.21 (2H, d, $J = 6.3$ Hz), 3.32 (3H, s), 1.51 (3H, s), 1.33 (3H, s); ^{13}C NMR (75 MHz, $CDCl_3$) δ_C: 169.9, 161.5, 155.1, 134.5, 134.3, 118.6, 116.1, 116.0, 112.9, 109.4, 85.1, 84.3, 81.4, 69.4, 55.1, 26.5, 25.0; CI-MS: 333 ($[M + 3]^+$), 330 ($[M]^+$), 241 ($[M-C_4H_9O_2]^+$); IR υ_{max} ($CHCl_3$)/cm^{-1}: 3028, 3018, 2989, 2246, 1367, 1218 1097.

2.1.6. Ribose-derived phthalonitrile **27**

White solid, yield (731 mg, 2.21 mmol, 55%); R_f 0.52 (hexane:ethyl acetate, 2:1); mp 123–125 °C; $[\alpha]_D$ −37.5° (*c* 0.144, $CHCl_3$); ^{1}H NMR (300 MHz, $CDCl_3$) δ_H: 7.70 (1H, d, $J = 8.7$ Hz), 7.26 (1H, d, $J = 2.4$ Hz), 7.20 (1H, dd, $J = 8.7$ and 2.7 Hz), 5.01 (H1, s), 4.73 (1H, d, $J = 5.4$ Hz), 4.62 (1H, d, $J = 6.0$ Hz), 4.51 (1H, t, $J = 7.1$ Hz), 4.05 (2H, m), 3.32 (3H, s), 1.49 (3H, s), 1.32 (3H, s); ^{13}C NMR (75 MHz, $CDCl_3$) δ_C: 161.2, 135.2, 119.4 (2C), 117.5, 116.0, 115.8, 112.8, 109.5, 107.9, 84.9, 83.9, 81.7, 69.3, 55.2, 26.4, 24.9; CI-MS: 315 ($[M - CH_3]^+$), 299 ($[M-OCH_3]^+$); IR υ_{max} ($CHCl_3$)/cm^{-1}: 3081, 2998, 2943, 2231, 1375, 1208, 1023.

2.1.7. Free-base phenoxy-substituted porphyrazine **32**

General route to the synthesis of free-base porphyrazines: A mixture of magnesium (120 mg, 5.00 mmol) and one small crystal of iodine in *n*-butanol (80 mL) was heated under reflux for 24 h 2,3-Dipropylmaleonitrile **30** (1.26 g, 7.77 mmol) and phenoxy-substituted phthalonitrile **16** (410 mg, 0.971 mmol) were added and the reaction mixture was heated for an additional 24 h. The mixture was allowed to cool to room temperature and the solvent was evaporated under reduced pressure. The crude mixture was dissolved in ethyl acetate and filtered to remove impurities. After evaporation of the solvent, the mixture was partially purified using

flash column chromatography on silica gel with gradient elution (hexane/ethyl acetate, 8:1, 3:1, 0:1). Magnesium ion was removed by overnight treatment of a DCM solution of the mixture with glacial acetic acid. The resulting blue solution was poured into ice-cold water (600 mL) and neutralised with an aqueous solution of sodium hydroxide (1 N). The precipitate that formed was filtered, washed with water, air dried and dissolved in dichloromethane. Purification was performed using flash column chromatography on silica gel (hexane/dichloromethane, 1:1). After evaporation of the solvent, the product was precipitated from methanol to yield **32** as a purple solid (207 mg, 0.227 mmol, 23%). R_f 0.14 (dichloromethane/hexane, 1:1); mp 169–172 °C; ^{1}H NMR (300 MHz, $CDCl_3$) δ_H: 8.74 (1H, s), 8.59 (1H, s), 7.41 (2H, t, J = 7.8 Hz), 7.25 (2H, d, J = 7.2 Hz), 7.12 (1H, t, J = 7.2 Hz), 5.10 (1H, s), 4.70 (1H, dd, J = 9.0 and 5.4 Hz), 4.61 (1H, d, J = 5.7 Hz), 4.58 (1H, dd, J_1 = 9.2 and 5.3 Hz), 4.53 (1H, d, J = 6.0 Hz), 4.38 (1H, t, J = 9.2 Hz), 3.80 (8H, m), 3.69 (4H, m), 3.49 (3H, s), 2.25 (12H, m), 1.54 (3H, s) 1.33 (3H, s), 1.26 (18H, m), −3.10 (2H, s); ^{13}C NMR (75 MHz, $CDCl_3$) δ_C: 161.8, 161.7, 158.9, 157.9, 157.5, 152.5, 146.6, 145.2, 144.9, 144.6, 144.5, 144.2, 143.9, 141.3, 141.2, 140.2139.8, 137.5, 134.3, 129.6 (2C), 122.4, 116.6 (2C), 116.0, 112.3, 109.8, 107.5, 85.2, 84.3, 81.9, 69.5, 55.0, 28.3, 28.1, 27.9 (2C), 26.5 (2C), 25.6 (2C), 25.5 (2C), 25.4 (2C), 25.0 (2C), 14.9 (3C), 14.8 (3C); UV–vis ($CHCl_3$) λ_{max} (log ε): 649 (5.09), 620 (4.04), 572 (5.05), 346 (5.13); FAB-MS: 910 ($[M-1]^+$).

2.1.8. Zinc-containing phenoxy-substituted porphyrazine **33**

General route for the metalation of porphyrazines with zinc: For **33**: To a solution of the free-base porphyrazine (70 mg, 0.077 mmol) in chlorobenzene (50 mL) and DMF (3 mL) was added $Zn(OAc)_2 \cdot 2H_2O$ (30 mg, 0.14 mmol). The mixture was heated to reflux overnight, after which it was cooled to room temperature and poured into ethyl acetate (300 mL). The reddish-purple solution was washed with water (100 mL × 3) and dried over anhydrous $MgSO_4$. After evaporation of the solvent, purification was performed using flash column chromatography by loading the sample onto the column with a dichloromethane/hexane mixture (1:1) followed by elution with dichloromethane/tetrahydrofuran (5:1). Further purification was achieved by precipitation of the metalated product from dichloromethane/methanol (63 mg, 0.065 mmol, 84%). R_f 0.33 (hexane/tetrahydrofuran, 1:10); mp 237–242 °C; ^{1}H NMR (300 MHz, $CDCl_3$) δ_H: 8.84 (1H, s), 8.56 (1H, s), 7.38 (2H, t, J = 7.3 Hz), 7.21 (2H, d, J = 7.8 Hz), 7.09 (1H, t, J = 7.2 Hz), 4.83 (1H, s), 4.46 (1H, d, J = 6.0 Hz), 4.43 (2H, d, J = 10.5 Hz), 4.37 (1H, d, J = 6.0 Hz), 4.26 (1H, t, J = 10.4 Hz), 3.58 (12H, m), 3.36 (3H, s), 2.12 (12H, m), 1.49 (3H, s), 1.43 (3H, s), 1.20 (18H, m); ^{13}C NMR (75 MHz, $CDCl_3$) δ_C: 158.7, 157.3, 156.8, 155.3, 155.1, 154.8, 152.9, 152.5, 152.4, 146.8, 144.3, 144.2, 144.1, 143.3, 143.2, 142.9, 142.4136.2, 133.0, 129.6 (2C), 122.4, 116.7 (2C), 115.9, 112.2, 109.5, 107.1, 85.0, 84.1, 81.7, 69.3, 54.8, 28.2, 28.0, 26.4 (2C), 25.6 (2C), 25.5 (2C), 25.4 (2C), 24.8 (2C), 22.7 (2C), 15.0 (3C), 14.9 (3C); UV–vis ($CHCl_3$) λ_{max} (log ε): 610 (4.00), 345 (4.13), 266 (3.71); FAB-MS: 974 ($[M]^+$).

2.1.9. Nickel-containing phenoxy-substituted porphyrazine **34**

General route to metalation of porphyrazines with nickel: For **34**: The free-base porphyrazine (55 mg, 0.061 mmol) was dissolved in chlorobenzene (30 mL). This was followed by addition of dry DMF (3 mL) and $Ni(OAc)_2 \cdot 4H_2O$ (26 mg, 0.11 mmol). The mixture was heated under reflux for 14 h, cooled to room temperature and poured into ethyl acetate (250 mL). The reddish-purple solution was washed with water (50 mL × 3) and dried over anhydrous $MgSO_4$. After evaporation of the solvent, purification was carried out using flash column chromatography by washing the sample onto the column with dichloromethane/hexane (1:1) followed by elution with neat dichloromethane. The product was precipitated from dichloromethane/pentane as a means of further purification to afford **34** as purple solid (51 mg, 0.052 mmol, 85%). R_f 0.21 (dichloromethane); mp 227–229 °C; ^{1}H NMR (300 MHz, $CDCl_3$) δ_H: 8.74 (1H, s), 8.52 (1H, s), 7.39 (2H, t, J = 7.2 Hz), 7.22 (2H, d, J = 7.8 Hz,), 7.12 (1H, t, J = 7.1 Hz), 5.08 (1H, s), 4.67 (2H, d, J = 8.7 Hz), 4.59 (1H, d, J = 6.0 Hz), 4.49 (1H, d, J = 6.0 Hz), 4.36 (1H, t, J = 8.7 Hz), 3.64 (12H, m), 3.48 (3H, s), 2.16 (12H, m), 1.53 (3H, s), 1.31 (3H, s), 1.23 (18H, m); ^{13}C NMR (75 MHz, $CDCl_3$) δ_C: 158.9 (2C), 152.8 (2C), 149.7, 149.3, 148.1, 147.8 (2C), 147.1, 146.1, 144.6, 144.5, 143.6, 143.4 (2C), 143.0, 135.4, 132.2, 129.7 (2C), 122.6, 116.8 (2C), 115.3, 112.4, 109.8, 106.3, 85.2, 84.2, 81.9, 69.4, 54.9, 29.7, 28.1 (3C), 27.9, 26.4, 25.5 (3C), 25.3, 25.2, 24.9, 14.8 (6C); UV–vis ($CHCl_3$) λ_{max} (log ε): 597 (4.38), 297 (4.38), 248 (4.35); FAB-MS: 968 ($[M]^+$).

2.1.10. Free-base ribose-substituted porphyrazine **36**

Chromatographed (hexane/dichloromethane, 2:3), purple solid (161 mg, 0.197 mmol, 23%); R_f 0.25 (hexane/dichloromethane, 2:3); mp 158–160 °C; ^{1}H NMR (300 MHz, $CDCl_3$) δ_H: 8.91 (1H, d, J = 6.9 Hz), 7.97 (1H, t, J = 7.7 Hz), 7.52 (1H, d, J = 8.1 Hz), 5.28 (1H, d, J = 5.7 Hz), 5.18 (1H, s), 4.82 (1H, d, J = 6.0 Hz), 4.73 (1H, m), 4.27 (2H, m), 3.97 (8H, m), 3.78 (4H, m), 3.46 (3H, s), 2.34 (12H, m), 1.61 (3H, s), 1.41 (3H, s), 1.26 (18H, m), −2.33 (2H, s); ^{13}C NMR (75 MHz, $CDCl_3$) δ_C: 162.5, 162.2, 158.8, 158.7, 155.2 (2C), 145.7, 145.6, 144.9, 144.8, 143.4, 141.7, 141.5, 141.1, 140.6, 130.8, 127.3, 116.2, 114.3, 112.5, 109.7, 85.4, 84.9, 82.7, 70.1, 55.2, 29.8 (2C), 28.3, 28.2, 28.1, 28.0, 27.8, 26.6, 25.5, 25.4 (2C), 25.3, 25.3, 25.1, 14.8 (3C), 14.7 (2C), 14.6; UV–vis ($CHCl_3$) λ_{max} (log ε): 654 (4.68), 577 (4.12), 327 (4.51); FAB-MS: 819 ($[M]^+$), 788 ($[M-OCH_3]^+$).

2.1.11. Zinc-containing ribose-substituted porphyrazine **40**

Chromatographed (hexane/acetone, 5:1), (52 mg, 0.059 mmol, 75%); R_f 0.16 (hexane/acetone, 5:1); mp 154–156 °C; ^{1}H NMR (300 MHz, $CDCl_3$) δ_H: 8.69 (1H, d, J = 6.9 Hz), 7.88 (1H, t, J = 7.5 Hz), 7.32 (1H, d, J = 7.8 Hz), 5.00 (1H, d, J = 5.4 Hz), 4.77 (1H, s), 4.71 (1H, t, J = 6.6 Hz), 4.59 (1H, d, J = 5.7 Hz), 4.41 (2H, d, J = 6.9 Hz), 3.78 (2H, m), 3.61 (6H, m), 3.43 (4H, s), 3.26 (3H, s), 2.21 (6H, m), 2.07 (6H, m), 1.49 (3H, s), 1.27 (9H, m), 1.25 (3H, m), 1.16 (9H, m); ^{13}C NMR (75 MHz, $CDCl_3$) δ_C: 158.1, 157.9, 156.5, 156.3, 155.2, 153.7, 153.6145.4, 144.3, 143.3, 143.1, 142.7, 141.9 (2C), 140.6, 130.3, 126.3, 116.1, 113.6, 112.6, 109.5, 85.1, 84.8, 82.3, 77.2, 69.9, 54.9, 29.6, 29.3, 28.4, 28.1, 27.9, 27.7, 27.0, 26.4, 25.5, 25.4, 25.3, 25.0, 24.9, 22.6, 14.9, 14.8 (2C), 14.7 (2C), 1.41; UV–vis ($CHCl_3$) λ_{max} (log ε): 617 (4.18), 343 (5.01), 264 (4.58); FAB-MS: 882 ($[M]^+$).

2.1.12. Nickel-containing ribose-substituted porphyrazine **44**

Chromatographic purification was performed using hexane/ethyl acetate (1:1), (60 mg, 0.069 mmol, 87%); R_f 0.15 (hexane/dichloromethane, 1:1); mp 169–173 °C; ^{1}H NMR (300 MHz, $CDCl_3$) δ_H: 8.69 (1H, d, J = 7.5 Hz), 7. 90 (1H, t, J = 7.7 Hz), 7.43 (1H, d, J = 8.1 Hz), 5.23 (1H, d, J = 5.7 Hz), 5.17 (1H, s), 5.15 (1H, t, J = 5.7 Hz), 4.81 (1H, d, J = 5.7 Hz), 4.65 (2H, m), 3.99 (1H, m), 3.68 (7H, m), 3.49 (4H, m), 3.47 (3H, s), 2.28 (6H, m), 2.11 (6H, m), 1.65 (3H, s), 1.41 (3H, s), 1.23 (18H, m); ^{13}C NMR (75 MHz, $CDCl_3$) δ_C: 154.8, 149.7, 149.2, 148.0, 147.9, 147.8, 147.7, 146.2, 146.1, 144.3, 144.2, 144.0, 143.4, 143.3, 142.9, 140.6, 130.2, 125.2, 115.2, 113.0, 112.6, 109.8, 85.4, 84.8, 82.8, 77.2, 69.8, 55.1, 29.6, 28.3, 28.0, 27.9, 27.8, 27.7, 27.6, 26.5, 25.5, 25.4, 25.3, 25.2 (2C), 25.0, 24.9, 14.9, 14.8 (2C), 14.7 (2C), 14.6; UV–vis ($CHCl_3$) λ_{max} (log ε): 604 (4.65), 315 (4.44), 291 (4.36); FAB-MS: 876 ($[M]^+$).

2.1.13. Free-base ribose-substituted porphyrazine **49**

Chromatographed (hexane/dichloromethane 1:3), purple solid (356 mg, 0.435 mmol, 26%); R_f 0.31 (hexane/dichoromethane, 1:3); mp 223–229 °C; ^{1}H NMR (300 MHz, $CDCl_3$) δ_H: 8.84 (1H, J = 8.1 Hz, d), 8.44 (1H, s), 7.52 (1H, d, J = 8.1 Hz), 5.18 (1H, s), 5.07 (1H, d, J = 6.0 Hz), 4.84 (1H, m), 4.48 (1H, d, J = 5.7 Hz), 4.50 (1H, t,

$J = 9.0$ Hz), 4.41 (1H, t, $J = 8.4$ Hz), 3.83 (8H, m), 3.69 (4H, m), 3.53 (3H, s), 2.23 (12H, m), 1.63 (3H, s), 1.45 (3H, s), 1.26 (18H, m), −2.68 (2H, s); ^{13}C NMR (75 MHz, $CDCl_3$) δ_C: 161.9, 161.6, 160.4, 158.9, 158.1, 145.7, 145.1, 144.6, 144.5, 144.4, 144.0, 142.3, 141.4, 141.3, 140.2, 139.9, 133.7, 123.4, 117.0, 112.7, 109.5, 106.8, 85.3, 84.9, 82.3, 69.1, 55.1, 29.8, 28.3, 28.1, 27.9, 26.6 (2C), 25.6 (2C), 25.5 (2C), 25.4 (2C), 25.2 (2C), 14.9 (3C), 14.8 (2C); UV–vis ($CHCl_3$) λ_{max} (log ε): 652 (5.23), 568 (4.96), 346 (5.02); FAB-MS: 819 ($[M]^+$).

2.1.14. Zinc-containing ribose-substituted porphyrazine ***54***

Chromatographed using tetrahydrofuran/dichloromethane (1:7), purple solid (69 mg, 0.078 mmol, 75%); R_f 0.29 (hexane/tetrahydrofuran, 6:1); mp 244–247 °C; ^{1}H NMR (300 MHz, pyridine-d_5) δ_H: 9.61 (1H, d, $J = 8.1$ Hz), 9.32 (1H, s), 7.96 (1H, d, $J = 8.1$ Hz), 5.39 (1H, s), 5.14 (1H, d, $J = 6.0$ Hz), 5.08 (1H, m), 4.97 (1H, d, $J = 5.7$ Hz), 4.67 (2H, m), 4.13 (12H, m), 3.49 (3H, s), 2.56 (12H, m), 1.65 (3H, s), 1.44 (3H, s), 1.36 (18H, m), ^{13}C NMR (75 MHz, pyridine-d_5) δ_C: 161.3, 159.8, 159.3, 157.7, 157.5, 157.3, 157.2, 156.0, 155.4, 144.8, 144.7, 143.7, 143.5, 143.4, 143.2, 142.4, 133.7, 124.6, 118.3, 112.7, 110.0, 107.7, 85.9, 85.3, 82.7, 70.2, 54.9, 30.0, 28.8, 28.6 (2C), 26.8 (2C), 26.3 (2C), 26.2 (2C), 26.1 (2C), 25.1 (2C), 15.2 (3C), 15.1 (3C); UV–vis ($CHCl_3$) λ_{max} (log ε): 609 (4.78), 343 (5.01), 264 (4.58); FAB-MS: 882 ($[M]^+$).

2.1.15. Nickel-containing ribose-substituted porphyrazine ***57***

Chromatographed using dichloromethane, purple solid (49 mg, 0.055 mmol, 64%); R_f 0.64 (dichloromethane); mp 237–240 °C; ^{1}H NMR (300 MHz, chlorobenzene-d_5, 50 °C) δ_H: 9.06 (1H, d, $J = 8.1$ Hz), 8.58 (1H, s), 7.36 (1H, d, $J = 8.1$ Hz), 4.91 (1H, s), 4.70 (1H, d, $J = 6.3$ Hz), 4.63 (1H, t, $J = 6.5$ Hz), 4.50 (1H, d, $J = 6.0$ Hz), 4.21 (1H, t, $J = 6.0$ Hz), 4.19 (1H, t, $J = 6.6$ Hz), 3.65 (12H, m), 3.17 (3H, s), 2.17 (12H, m), 1.32 (3H, s), 1.14 (3H, s), 1.11 (18H, m); ^{13}C NMR 75 MHz, Chlorobenzene-d_5, 50 °C) δ_C: 160.5 (2C), 148.4 (2C), 147.9, 144.9 (2C), 143.7 (2C), 143.5 (2C), 123.8, 118.3, 112.8, 109.7, 105.5, 85.3, 84.9, 82.3, 69.2, 55.0, 28.2 (2C), 26.6 (6C), 25.5 (3C), 25.1 (3C), 14.8 (6C); UV–vis ($CHCl_3$) λ_{max} (log ε): 598 (4.62), 293 (4.46); FAB-MS: 874 ($[M - 2]^+$)

2.1.16. Deprotected phenoxy-substituted porphyrazine ***61***

General route for the isopropylidene-deprotection of free-base porphyrazines using methanol: For **61**, **32** (42 mg, 0.042 mmol) was dissolved in THF (25 mL), followed by the addition of MeOH (5 mL) and a catalytic amount of *p*-TsOH. The ensuing reaction mixture was heated to 75–78 °C for 48 h (TLC monitoring), after which the mixture was quenched by cooling to room temperature. The crude product was dissolved in ethyl acetate (200 mL), washed successively with an aqueous sodium hydrogen carbonate solution (20 mL × 3), water (20 mL × 3), dried with $MgSO_4$ and concentrated. Flash chromatography (hexane/ethyl acetate, 2:1) followed by precipitation (hexane/ethyl acetate) gave (14 mg, 0.016 mmol, 36%). R_f 0.15 (hexane/ethyl acetate, 2:1); mp 232–238 °C; UV–vis (2-Octanol) λ_{max} (log ε): 670 (4.90), 600 (4.86), 580 (4.79), 390 (4.84); MS-FAB: 870.0 ($[M + 1]^+$).

2.1.17. Deprotected glucose-substituted porphyrazine ***62***

General route to the isopropylidene-deprotection of free-base porphyrazines using methanol and water: For **62**, to a stirred solution of **36** (50 mg, 0.057 mmol) in THF (40 mL) was added MeOH/H_2O (2 mL:1.5 mL) and a catalytic amount of *p*-TsOH. The mixture was heated to 50–55 °C overnight, after which it was poured into ethyl acetate (300 mL) and neutralised with an aqueous sodium hydrogen carbonate solution (20 mL × 3). It was washed with water (20 mL × 3), dried with $MgSO_4$ and concentrated. Chromatographic separation (hexane/ethyl acetate, 3:1) followed by precipitation (DCM/MeOH) yielded **62** (37 mg, 0.044 mmol, 77%). R_f 0.29 (hexane/dichloromethane, 3:1), mp 186–190 °C; ^{1}H NMR (300 MHz, $CDCl_3$) δ_H: 8.95 (1H, d, $J = 7.5$ Hz), 8.02 (1H, t, $J = 7.7$ Hz), 7.67 (1H, d, $J = 7.8$ Hz), 6.32 (1H, d, $J = 3.9$ Hz), 5.66 (1H, d, $J = 3.3$ Hz), 5.02 (2H, m), 4.72 (1H, dd, $J = 7.4$ and 3.2 Hz), 4.11 (2H, m), 3.94 (12H, m), 2.30 (12H, m), 1.66 (3H, s), 1.54 (2H, s br), 1.36 (3H, s), 1.25 (18H, m), −2.25 (2H, s): ^{13}C NMR (75 MHz, $CDCl_3$) δ_C: 163.1, 162.3, 158.3, 158.0, 153,1 145.6, 145.3, 145.2 (2C), 144.9, 144.4, 143.6, 141.9, 141.7, 140.9, 140.8, 130.9, 127.4, 116.6, 113.7, 112.3, 105.6, 82.7, 81.6, 79.8, 69.8, 64.8, 29.7 (3C), 29.4, 28.3, 28.0, 27.9, 27.4, 26.9, 26.4, 25.6 (2C), 25.5, 25.3, 14.9 (2C), 14.8 (2C), 14.3, 14.2; UV–vis (2-Octanol) λ_{max} (log ε): 655 (5.10), 577 (5.05), 327 (4.97); FAB-MS: 835 ($[M]^+$).

2.2. Measurement of partition coefficients

A typical experiment was performed as follows: The porphyrazine derivative (7 mg) was dissolved in 2-octanol (10 mL), which was stirred at room temperature for 12 h. The solution was filtered using a sintered glass funnel, to remove any undissolved porphyrazine. This was followed by addition of PBS solution (10 mL) and the mixture was stirred for the next 8–12 h. The two layers were allowed to separate (3 min). Aliquots of the aqueous (10 mL) and organic layers (0.5–2 mL), were taken. The aqueous layer was diluted to 20 mL with 2.0 M solution of HCl in THF. The organic layer was treated with PBS (8–9.5 mL) and then diluted to 40–70 mL with a 2.0 M solution of HCl in THF. Electronic spectra were measured (300–700 nm), using 1 cm path length glass cuvettes. The absorbances were taken from the Soret band region as well as the red band region. The partition coefficients were calculated using equation (4). The measurements were carried out in triplicate.

3. Results and discussion

3.1. Carbohydrate synthesis

For the purpose of this study, any protecting groups on the carbohydrate would have to be base-stable in order to withstand the Linstead macrocyclisation conditions ($Mg(OBu)_2$, *n*-BuOH, reflux). Several protecting groups, such as acetals, show this base-resistance and were therefore deemed suitable for our purposes [23]. Accordingly, acetonide-protected D-(−)-ribose **9** was used in coupling reactions with phthalonitriles as described below.

Disaccharides were also of interest for this study but there are limited numbers and types of commercially available disaccharides. In the present study, it was important to be able to prepare disaccharides such that (i) one hydroxyl group remained unmasked or could be selectively deprotected and (ii) the protecting groups would be resistant to the Linstead macrocyclisation conditions. 1:2,3:4-Di-*O*-isopropylidene-D-galactopyranose **4** was selected as a suitable commercially available starting material. Disaccharide synthesis was carried out as shown in Scheme 1, following several protection/deprotection steps and other functional group transformations.

The disaccharides were synthesised by using galactosyl bromide **3** [24] as the glycosyl donor and **4** or **9** as the glycosyl acceptor, in the presence of Ag_2CO_3 and molecular sieves. The products **5** and **10**, respectively, were purified and deprotected of their acetyl groups using triethylamine in methanol at 40 °C. MOM protection (to provide base-stable groups referred to earlier) of the partially protected disaccharides **6** or **11** with chloromethyl methyl ether in the presence of a base (Scheme 2) afforded the desired products **7** and **12** in yields of 90% and 88%, respectively. Removal of the benzyl group by hydrogenolysis (10% Pd/C, 350 kPa hydrogen pressure) finally yielded the disaccharides **8** (91%) or **13** (73%) with one free

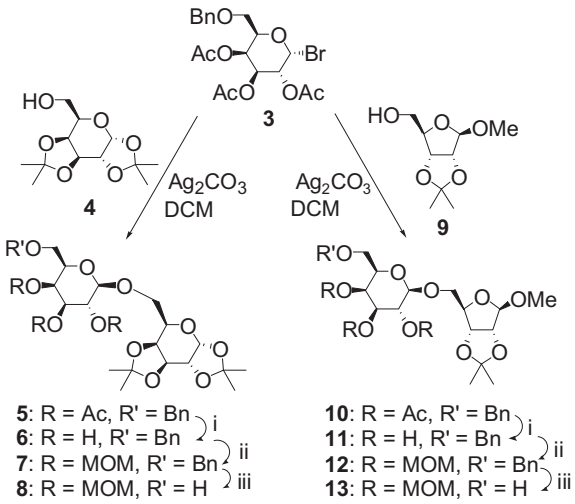

Scheme 1. Synthesis of disaccharide carbohydrates. i) Et_3N, MeOH, 40 °C; ii) NaH, THF, MOMCl; iiii) Pd/C, H_2, MeOH.

hydroxyl group, which could be used in coupling reactions with the phthalonitrile.

3.2. Phthalonitrile synthesis

4,5-Dichlorophthalonitrile **14** was coupled with protected ribose **9** in the presence of potassium carbonate in DMSO to give compound **15** in 40% yield (Scheme 2).

Even though 2 equivalents of carbohydrate were used in the reaction, only the mono carbohydrate-substituted phthalonitrile **15** was obtained in moderate yield even after prolonged heating. It is probable that the second substitution failed due to steric hindrance. The product was crystallised from DCM by trituration with methanol and was collected as white needle-shaped crystals. Despite the lack of reactivity in the presence of an excess of **9**, product **15** could be made to react with phenol to afford compound **16** as white crystals after crystallisation from DCM by trituration with MeOH. A reversal of this coupling reaction afforded only the diphenoxy substituted phthalonitrile.

The use of a nitro moiety as a leaving group on a phthalonitrile substrate required different conditions compared to the use of chloro leaving groups, as was established after some experimentation. Four different functionalised carbohydrates, namely **4**, **9**, **20** and **22**, were coupled with phthalonitrile **17** using NaH or K_2CO_3 as base in DMF to give the corresponding phthalonitrile adducts **18** (33%, NaH as base), **19** (57%, K_2CO_3 as base), **21** (71%, K_2CO_3 as base) and **23** (80%), respectively (Scheme 3). Presumably, the free amine

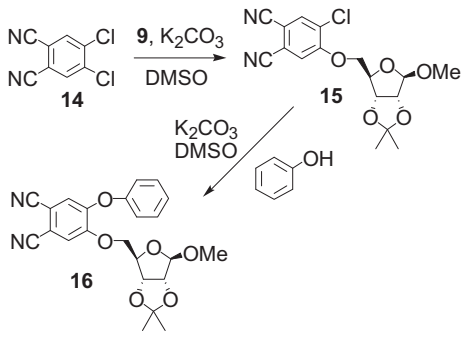

Scheme 2. Selective functionalisation of 4,5-dichlorophthalonitrile.

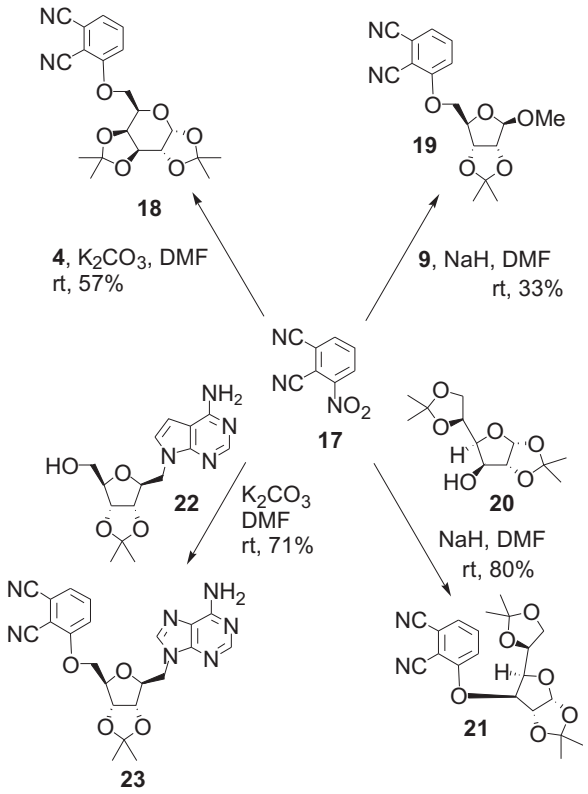

Scheme 3. Synthesis of 3-carbohydrate-functionalised phthalonitriles.

of **22** fails to react with the otherwise susceptible nitrophthalonitrile substrate (**17**, here, and **24**, below) due to its significantly lowered nucleophilicity, it being an aromatic amine on an aromatic heterocycle. It is in all likelihood the same reasoning that accounts for the absence of amidine formation during the macrocyclisation reactions of products **23** and **26**, the reactions of which are detailed below in Schemes 6 and 7, to produce macrocyclic structures **38**, **42**, **46**, **48**, **53** and **56,** respectively.

Functionalisation of **24** with each of five carbohydrate derivatives was achieved through the use of selectively protected carbohydrates with primary hydroxyl groups as nucleophiles to afford the various products in moderate yields (18–66%). In each coupling reaction, the phthalonitrile was added to a suspension of the carbohydrate and potassium carbonate in DMF (Scheme 4) to provide products **25** (52%), **26** (52%), **27** (55%), **28** (48%) and **29** (79%) as pure products after column chromatography. The large difference in the yields for **28** and **29**, which are structurally similar products, is not understood but was consistently observed through several repeat reactions.

3.3. Synthesis, deprotection and metalation of porphyrazines

In the synthesis of the functionalised porphyrazines (Schemes 6–8), 8–15 equivalents of 2,3-dipropylmaleonitrile **30** were reacted with each carbohydrate-substituted phthalonitrile (1 equivalent), respectively, by heating each mixture under reflux in *n*-butanol in the presence of $Mg(OBu)_2$ for 24 h. The magnesium-complexed product obtained from each reaction was partially purified by flash column chromatography using hexane/ethyl acetate mixtures as the eluent to afford reddish-blue Mg-complexed products at >80% purity. Removal of the central magnesium ion was effected using glacial acetic acid at room temperature by dissolving each porphyrazine in DCM followed by the addition of

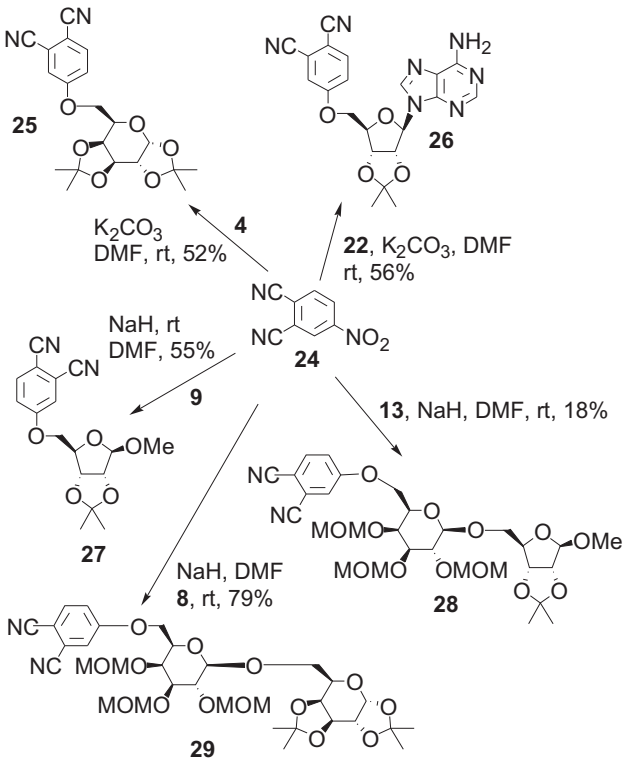

Scheme 4. Synthesis of 4-carbohydrate-functionalised phthalonitriles.

acetic acid, and the reaction mixture was stirred overnight. Chromatography provided the pure free-base macrocycles.

The porphyrazines of this study were metalated with both nickel and zinc by reaction thereof for 16 h with the metal acetate salts in a mixture of chlorobenzene and DMF, the ratio of which depended on the porphyrazine solubility in chlorobenzene. At temperatures of about 100 °C or lower, products were obtained in low yields (i.e., <50%), the consequence of which is that the reactions were performed at temperatures above 100 °C. The porphyrazine complexes could be purified by column chromatography, which was sometimes complicated due to the low solubility of the nickel complexes in most organic solvents.

Reaction of 8 equivalents of maleonitrile **30** with **16** gave the magnesium complex **31** which was partially purified by chromatography (Scheme 5). Further manipulations as described above provided **32** (M = 2H, 23%, blue amorphous solid), **33** (M = Zn, 84%, red-purple amorphous solid) and **34** (M = Ni, 85%, red-purple amorphous solid).

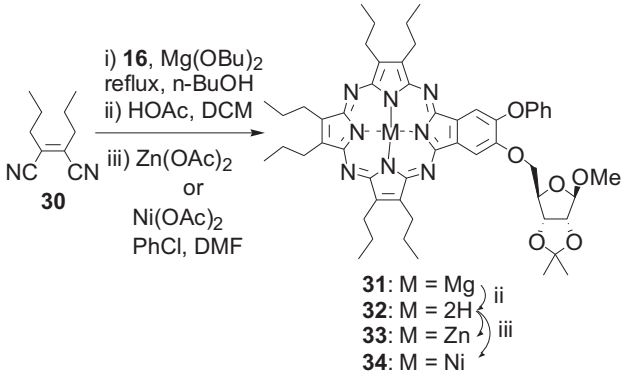

Scheme 5. Synthesis of ribose-derived porphyrazine.

Similarly, free-base porphyrazines **35**–**38**, shown in Scheme 6, were prepared by reaction of 6–8 equivalents of **30** with each carbohydrate-substituted phthalonitrile **18**, **19**, **21** and **23**, respectively. After removal of the central metal ion, the products were precipitated from methanol and collected as blue precipitates to yield **35** (23%), **36** (37%), **37** (12%) and **38** (30%).

Metalation of free-base pigments **35**–**38** with $Zn(OAc)_2 \cdot 2H_2O$ or $Ni(OAc)_2 \cdot 4H_2O$ afforded metalated porphyrazines **39**–**46** (Scheme 6). Precipitation of the complexes from appropriate solvents proved the method of choice to provide analytically pure products. Lower yields were obtained for both **39** and **43**, which were synthesised from **35**. Both of these compounds easily decomposed during evaporation of the solvent and also under conditions under which they were synthesised. When the metal insertion was carried out at temperatures between 70 °C and 100 °C, the yields were lower than 50% due to incomplete conversion of the substrate to product. At higher temperatures, the products decomposed.

Pigments **47**–**51** were similarly prepared (Scheme 7) and purified by chromatography and precipitation from methanol (**47**, 26%; **48**; 28%; **49**; 18%; **50**, 8%; **51**, 22%). The low yield of **50** resulted due to the dipropylmaleonitrile being consumed faster than the phthalonitrile derivative, because of their differential reactivity, resulting in less of the dipropylmaleonitrile coupling with the phthalonitrile adduct.

The zinc- and nickel-metalated derivatives of **47**–**49** were prepared from the metal acetate salts using the protocols described above, to provide **52** (81%), **53** (51%), **54** (75%), **55** (64%), **56** (63%) and **57** (63%). Precipitation was again most useful approach to assist in purification of the materials. With complex **56**, precipitation was

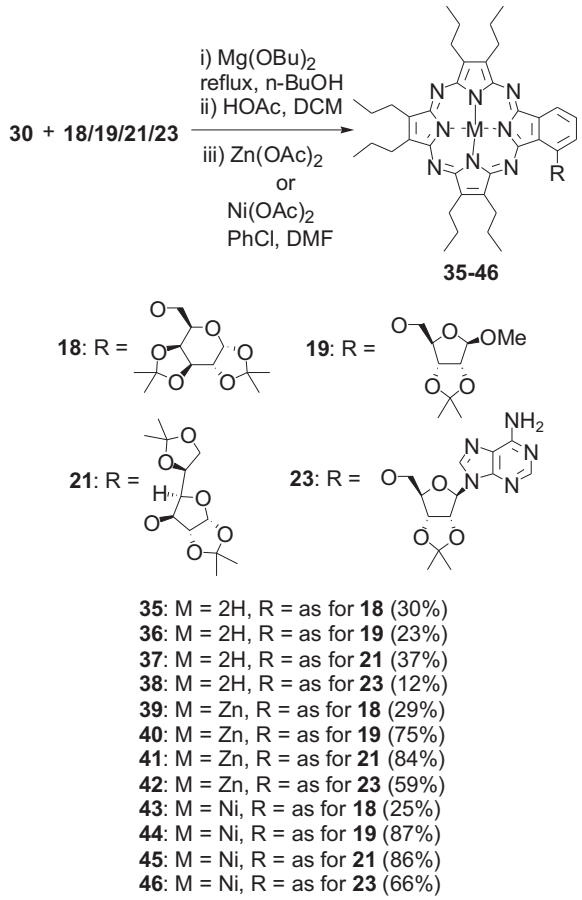

Scheme 6. Synthesis of carbohydrate-functionalised porphyrazines.

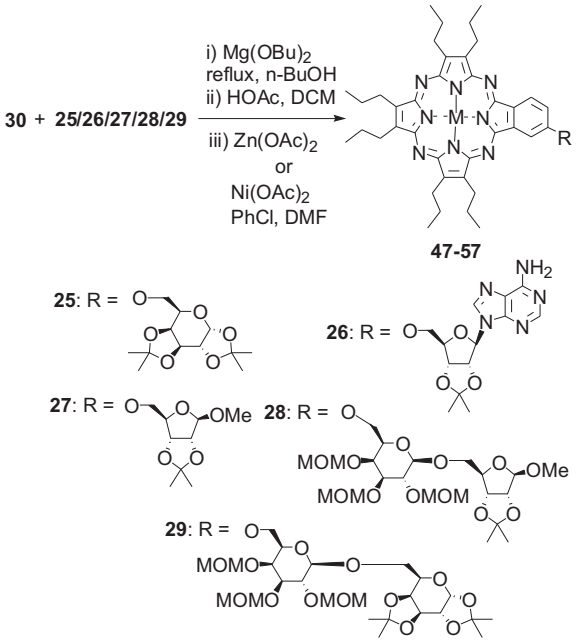

47: M = 2H, R = **25** (28%)
48: M = 2H, R = **26** (8%)
49: M = 2H, R = **27** (26%)
50: M = 2H, R = **28** (18%)
51: M = 2H, R = **29** (22%)
52: M = Zn, R = **25** (81%)
53: M = Zn, R = **26** (51%)
54: M = Zn, R = **27** (75%)
55: M = Ni, R = **25** (64%)
56: M = Ni, R = **26** (63%)
57: M = Ni, R = **27** (64%)

Scheme 7. Synthesis of carbohydrate-functionalised porphyrazines.

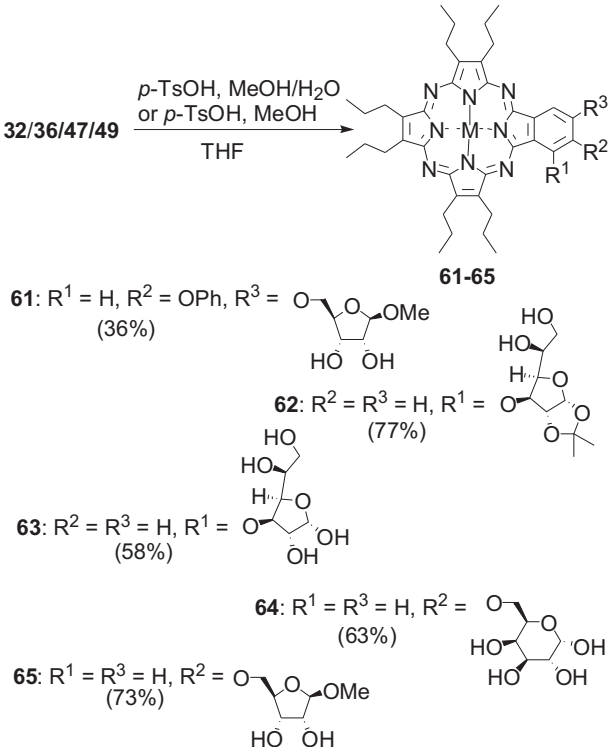

Scheme 8. Deprotection of carbohydrate-functionalised porphyrazines.

carried out using methanol, but this macrocycle was virtually insoluble in every organic solvent.

As one of the objectives of this study, deprotection of the synthesised porphyrazines was to be performed. Deprotection of the carbohydrate-functionalised compounds was anticipated to increase their solubility in aqueous media. The deprotection transformation of compounds **32**, **36**, **47** and **49** (Scheme 8) in aqueous- or in neat methanol, depending on the desired selectivity for the group to be deprotected, was effected using *p*-TsOH (*p*-toluenesulfonic acid). Each porphyrazine was dissolved in a suitable amount of THF, followed by addition of neat MeOH or aqueous MeOH and the sulfonic acid and the mixture was then heated. Deprotection was performed at elevated temperatures since no deprotection at all was observed at room temperature even after extended periods of time, which may relate to the solubility of the parent compounds in the reaction mixture. The temperature was found to be critical for each reaction such that a slight increase or decrease of the temperature negatively affected the yield. Porphyrazines **61**–**65**, all of which were cleaved of their isopropylidene acetal protecting groups, were poorly soluble in all solvents tested and could therefore not be characterised using NMR spectroscopy (but for **62**).

The nature of the insoluble products was tentatively confirmed by FAB-MS (low resolution) which showed the expected molecular ion peaks. Gratifyingly, compound **62** was fairly soluble and could be analysed using FAB-MS, ^{1}H NMR and ^{13}C NMR spectroscopy. FAB-MS analysis exhibited peaks for **61** at *m*/*z* 870 ($[M-1]^+$), for **62** at *m*/*z* 835.4 ($[M]^+$), for **63** at *m*/*z* 796 ($[M+1]^+$), for **64** at *m*/*z* 796 ($[M+1]^+$) and for **65** at *m*/*z* 779 ($[M]^+$), all of which were the anticipated signals.

In the case of porphyrazine **32**, this material was protected by a methyl and an isopropylidene acetal on the D-(−)-ribose residue. Both of these groups are potentially cleavable under acidic conditions. To prevent mixtures of partially and fully deprotected products, neat MeOH was used instead of using aqueous methanol, as shown in Scheme 8. This approach very effectively ensured retention of the 1-*O*-methyl protecting group when heating for two days at 75–78 °C. The diol product **61**, which was precipitated from a mixture of hexane and ethyl acetate, was collected as a purple precipitate in 36% yield.

Compound **36** was selectively deprotected by heating a mixture thereof in THF/MeOH/H_2O (40:2:1.5, v/v/v) and *p*-TsOH at 50–55 °C for 12–14 h to give **62**, which was collected in 77% yield as a blue precipitate from methanol. Raising the temperature to 75 °C allowed deprotection of the second isopropylidene acetal to give **63** as a mixture, after running the reaction for up to three days, with small amounts of **62** remaining. Deprotected porphyrazine **63** was collected as blue precipitate in 58% after treatment of pigment **62** with *p*-TsOH in aqueous MeOH. For diol **62**, disappearance of only two of the four high-field methyl singlet signals in the ^{1}H NMR spectrum of the product clearly indicated the removal of one isopropylidene acetal group only.

Compound **47** was treated with MeOH/H_2O (1:1 v/v) for three to four days in the presence of *p*-TsOH. The product **64** was collected in 63% yield after precipitation from DCM. For this reaction, the temperature was controlled at 75–80 °C. Heating the mixture at temperatures outside of this range lowered the yield or failed altogether to effect any reaction at all. Compound **64** was collected as a mixture of anomers, as is expected for a free sugar which is present as a mixture of α and β isomers. In a similar way, compound **65** could be obtained from its parent molecule **49** in a yield of 73% yield after precipitation from DCM.

3.4. Electronic absorption spectra

The UV–visible spectra for the free-base porphyrazines in the present study demonstrate generic Soret and Q-Band features strongly resembling those of unsymmetrical porphyrazine or phthalocyanine analogues. Porphyrazines **32**, **35**–**38**, **47**–**51** and **61**–**65**, which are all free-base porphyrazines, exhibit Soret absorption maxima between 325 and 348 nm and a split Q-band, having Q_x and Q_y absorbances at 571–580 nm and 649–656 nm, which is distinctive of unsymmetrical (D_{2h} symmetry) free-base tetraazaporphyrins. Gouterman's simplified four molecular orbital models for porphyrinic macrocycles provides a qualitative description of this phenomenon [25–29]. Generally, removal of magnesium metal or any metal at the centre reduces the symmetry which leads to splitting of the Q-band giving rise to two distinct absorbances, Q_x and Q_y, while the introduction of a metal increases the symmetry. For compound **32**, the Soret band is accompanied by an absorption peak that is higher in energy, which could be contributed by phenoxy group.

The metalated Ni(II) and Zn(II) derivatives (**40**–**46** and **52**–**57**) show two intense $\pi \rightarrow \pi^*$ absorbances: a low-energy Q band was present at 596–611 nm, which is accompanied by a slightly higher energy shoulder, and a high energy B band at 290–350 nm. For metalated porphyrazine derivatives, the symmetry of the π-chromophore is D_{4h} with the two LUMOs (b_{2g} and b_{3g}) giving rise to a two-fold degenerate e_g level, with the resulting spectra providing unsplit Q and B absorptions associated with transitions $a_{1u} \rightarrow e_g$ and $a_{2u} \rightarrow e_g$ as expected in metalated products [30]. However, the Soret bands are broad, which could arise because of some overlapping $\pi \rightarrow \pi^*$ and $n \rightarrow \pi^*$ transitions. When compared to their precursors, the Soret bands and Q-bands are blue shifted for both nickel and zinc complexed compounds. The Q-bands demonstrate similar features in all these porphyrazines, i.e., they are single intense bands with shoulders at slightly higher energy.

3.5. Partition coefficients

The partition coefficients of the protected and non-protected compounds were measured between 2-octanol and aqueous phosphate buffered saline (PBS) and compared to non-carbohydrate-substituted pigments. The porphyrazines analysed in the present study frequently displayed limited solubility in 2-octanol, although sufficient of each pigment dissolved in order to perform the experiments (given their high extinction coefficients, only small amounts are required to solubilise in order to obtain accurate data). Each porphyrazine was dissolved in 10 mL of 2-octanol by stirring for 8–12 h. Undissolved material was filtered and PBS solution (10 mL) was added and the mixture was vigorously stirred for 12 h after which the two layers were separated and analysed. The concentration of each solution was accurately determined making use of extinction coefficients as calculated from results of the present study (in, for example, DCM), together with UV–visible absorption data (see Table 1). The analysis of the aqueous layer required relatively large samples (10 mL) because of the very low concentrations of most of the porphyrazines studied in the aqueous layers at the *p*H value of 7.4. These samples were then dissolved in a 2.0 M solution of HCl in THF (10 mL). Small amounts (0.5–2.0 mL) of the organic phase were diluted with appropriate quantities of the acidic THF solution and the aqueous buffer system to bring the organic phase samples to conditions identical to those under which the aqueous phase samples were measured. All electronic spectrophotometric measurements were carried out using 1 cm path length cells. The absorbances as measured were used in subsequent calculations of the partition coefficients, starting with the formula shown in equation (1), which, after manipulation, derived to the formula shown in equation (4).

Table 1
Partition coefficients of porphyrazines.

Compound	$C(M)^{1a}$	K_{ow}^{2b}
1	9.427×10^{-3}	1.21×10^{4}
2	8.821×10^{-3}	1.01×10^{4}
32	5.488×10^{-3}	1.74×10^{3}
35	5.714×10^{-3}	1.61×10^{3}
36	6.104×10^{-3}	4.35×10^{3}
37	5.714×10^{-3}	1.27×10^{3}
38	5.422×10^{-3}	1.26×10^{3}
47	5.714×10^{-3}	1.75×10^{3}
48	5.422×10^{-3}	9.05×10^{2}
49	6.104×10^{-3}	5.40×10^{2}
50	5.422×10^{-3}	1.79×10^{3}
51	5.986×10^{-3}	3.09×10^{3}
61	4.592×10^{-3}	2.82×10^{2}
62	4.711×10^{-3}	5.07×10^{2}
63	5.032×10^{-3}	2.31×10^{2}
64	5.032×10^{-3}	4.20×10^{2}
65	4.884×10^{-3}	1.62×10^{2}

[a] C: Concentration in 2-octanol.
[b] K_{ow}: Octanol–water partition coefficient 1.

$$P = \frac{A(\text{org}) \times d(\text{org})}{A(\text{aq}) \times d(\text{aq})} \quad (1)$$

where A(org) is the absorbance of the organic layer, A(aq) is the absorbance of the aqueous layer, d(org) is the dilution factor for the organic layer, and d(aq) is the dilution factor for the aqueous layer. The dilution factor is the ratio of the final volume of the sample to the volume of aliquot according to equations (2) and (3):

$$d(\text{org}) = \frac{Vf(\text{org})}{V(\text{org})} \quad (2)$$

$$d(\text{aq}) = \frac{Vf(\text{aq})}{V(\text{aq})} \quad (3)$$

where Vf(org) is the final volume of the sample from the organic layer, V(org) is the volume of the aliquot from the organic layer, Vf(aq) is the final volume of the sample from the aqueous layer, V(aq) is the volume of the aliquot of the aqueous layer. Substitution of equations (2) and (3) into 1 gives equation (4), which is the equation used to calculate the partition coefficients.

$$P = \frac{A(\text{org}) \times Vf(\text{org}) \times V(\text{aq})}{A(\text{aq}) \times V(\text{org}) \times Vf(\text{aq})} \quad (4)$$

The concentrations of porphyrazines **1**, **2**, **32**, **35**–**38**, **47**–**51** and **61**–**65** in 2-octanol and their partition coefficients are listed according to the carbohydrate and its position of attachment. However, the first two porphyrazines listed include no carbohydrate substituents. Compounds **1** and **2** were used as non-functionalised and functionalised porphyrazine benchmarks, respectively. The first carbohydrate-substituted porphyrazine is **32** with the carbohydrate residue attached at position 4 and having a phenoxy group in position 5. The next four porphyrazines have the carbohydrate located in position 3 (**35**–**38**), while the next three porphyrazines listed have their monosaccharide residues in position 4 (**47**–**49**) and the two porphyrazines with the disaccharides located in position 4 (**50** and **51**) are shown last.

Porphyrazines **61**–**65** are deprotected porphyrazines having their isopropylidene acetal cleaved and they have different carbohydrates at different positions. All compounds tested demonstrated improved solubility in the aqueous phase over the test compounds.

The results tabulated in Table 1 and shown in Fig. 1 illustrate a one to two orders of magnitude decline of the partition coefficients into 2-octanol (corresponding to improved water solubility) with carbohydrate attachment, when compared to non-carbohydrate-substituted porphyrazines **1** and **2**. The partition coefficients for porphyrazines **1** and **2** are in the region of $1.01–1.21 \times 10^4$ whereas those of carbohydrate-substituted porphyrazines **35**–**38** and **47**–**51** clearly indicate higher water solubility. The results show that there is no clear or strong trend connecting to either the carbohydrate or the position of attachment of the carbohydrate onto the benzo ring to the extraction coefficients, save that all of these compounds demonstrated improved water solubilities over their unfunctionalised counterparts.

Notwithstanding the above generalised statements, porphyrazines with carbohydrates at position 3 all afforded slightly elevated partition coefficients compared to the ones with carbohydrate in position 4, with the exception of porphyrazines **36** and **48**, which demonstrated essentially identical partition coefficients. When comparing pigments **32** (contains the OPh group) and **47** (no OPh group), it is clear that the presence of the phenoxy group results in a product of higher oil/fat solubility, as expected. Using disaccharides as substituents did not improve the water solubility when compared to porphyrazines with monosaccharides as substituents. However, it was thought likely that a substantially different picture would emerge should these products be deprotected. Deprotection of the isopropylidene acetal groups resulted in a lowering of the partition coefficients, with the hydrophilic character increasing in these porphyrazines compared to their precursors (Table 1). Here too, there is also no clear trend with regard to the deprotected porphyrazines but they all showed improved water solubility compared to their protected counterparts. For porphyrazine **38**, the increase in the number of hydroxyl groupswith each deprotection step causes significant changes to the partition coefficients with the trend on the partition coefficient decreases as follows, **38** > **63** (2OH) > **64** (4OH), indicative of an increased water solubility concomitant with each deprotection step, as would be expected.

4. Conclusions

Overall, this study has demonstrated the successful incorporation of carbohydrate derivatives into phthalonitrile substrates and the use thereof in the synthesis of carbohydrate-functionalised porphyrazines. The products were successfully metal-deprotected to afford the free-base analogues, from which the corresponding Zn- or Ni complexes could be prepared. Additionally, the carbohydrate moieties could be deprotected to unmask the hydroxyl groups, the effect of which was to further enhance the water solubility imparted by the presence of the carbohydrate residues. This study bodes well for future work in this area.

The presence of carbohydrate substituents in each porphyrazine caused marked increases in the hydrophilicity of these complexes. Deprotection to reveal the hydroxyl groups further increased the hydrophilicity by two orders of magnitude (10^2). The effect of metalation was highly pronounced in the UV–visible characterisation studies, with metalation in the porphyrazine cavity causing some blue shift which was significant in the Soret region in all metalated porphyrazines.

Acknowledgements

The authors thank the National Research Foundation of South Africa, Medical Research Council of South Africa and the University of Johannesburg for funding.

Appendix. Supplementary data

Supplementary data associated with this article can be found, in the online version, at doi:10.1016/j.dyepig.2010.05.002.

References

[1] Fitzgerald JP, Haggerty BS, Rheingold AL, May L, Brewer GA. Iron octaethyltetraazaporphyrins: synthesis, characterization, coordination chemistry, and comparisons to related iron porphyrins and phthalocyanines. Inorganic Chemistry 1992;31:2006–13.
[2] Stuzhin PA, Hamdush M, Ziener U. Iron octaphenyltetraazaporphyrins: synthesis and characterization of the five-coordinate complexes of iron (III) (XFe^{III}OPTAP; X = F, Cl, Br, I, and HSO_4). Inorganic Chimica Acta 1995;236:131–9.
[3] Ni Y, Fitzgerald JP, Carroll P, Wayland BB. Formation and reactivity of (octaethyltetraazaporphyrinato)rhodium complexes. Inorganic Chemistry 1994;33:2029–35.
[4] Cosimelli B, Roncucci G, Dei D, Fantetti L, Ferroni F, Ricci M, et al. Synthesis and antimycotic activity of new unsymmetrical substituted zinc phthalocyanines. Tetrahedron 2003;59:10025–30.
[5] Kubát P, Mosinger J. Photophysical properties of metal complexes of meso-tetrakis(4-sulfonatophenyl)porphyrin. Journal of Photochemistry and Photobiology A: Chemistry 1996;96:93–7.
[6] Li G, Pandey SK, Graham A, Dobhal MP, Mehta R, Chem Y, et al. Functionalization of OEP-based benzochlorins to develop carbohydrate-conjugated photosensitizers. Attempt to target β-galactoside-recognized proteins. Journal of Organic Chemistry 2004;69:158–72.
[7] Montalban AG, Jarrell W, Riguet E, McCubbin QJ, Anderson ME, White AJP, et al. Bis(dimethylamino)porphyrazines: synthetic, structural, and spectroscopic investigations. Journal of Organic Chemistry 2000;65:2472–8.
[8] Freyer W, Flatau S. The first annulated porphyrazine containing four endoperoxide bridges. Tetrahedron Letters 1996;37:5083–6.
[9] Sakellariou EG, Montalban AG, Beall SL, Henderson D, Meunier HG, Phillips D, et al. Novel peripherally functionalized seco-porphyrazines: synthesis, characterization and spectroscopic evaluation. Tetrahedron 2003;59:9083–90.
[10] Sakellariou EG, Montalban AG, Meunier HG, Ostler RB, Rumbles G, Barrett AGM, et al. Synthesis and photophysical properties of peripherally metalated bis(dimethylamino)porphyrazines. Journal of Photochemistry and Photobiology A Chemistry 2000;136:185–7.
[11] Montalban AG, Meunier HG, Ostler RB, Barrett AGM, Hoffman BM, Rumbles G. Photoperoxidation of a diamino zinc porphyrazine to the seco-zinc porphyrazine: suicide or murder? Journal of Physical Chemistry A 1999;103:4352–8.
[12] Sakellariou EG, Montalban AG, Meunier HG, Rumbles G, Phillips D, Ostler RB, et al. Peripherally metalated secoporphyrazines: a new generation of photoactive pigments. Inorganic Chemistry 2002;41:2182–7.
[13] Kaiser AB, Kernoble DS. Synergism between poly-(1-6)-β-D-glucopyranosyl-(1-3)-β-D-glucopyranose glucan and cefazolin in prophylaxis of staphylococcal wound infection in a guinea pig model. Antimicrobial Agents and Chemotherapy 1998;42:2449–51.
[14] Williams PAM, Etcheverry SB, Barrio DA, Baran EJ. Synthesis, characterization, and biological activity of oxovanadium(IV) complexes with polyalcohols. Carbohydrate Research 2006;341:717–24.
[15] Shiozaki M, Iwano Y, Doi H, Tanaka D, Shimozato T, Kurakata S. Syntheses of glucose derivatives of E5564-related compounds and their LPS-antagonistic activities. Carbohydrate Research 2006;341:811–22.
[16] Chandrasekaran EV, Xue J, Neelamegham S, Matta KL. Syntheses of glucose derivatives of E5564-related compounds and their LPS-antagonistic activities. Carbohydrate Research 2006;341:983–94.
[17] Zheng X, Morgan J, Pandey SK, Chen Y, Tracy E, Baumann H, et al. Conjugation of 2-(1′-hexyloxyethyl)-2-devinylpyropheophorbide-a (HPPH) to carbohydrates changes its subcellular distribution and enhances photodynamic activity in vivo. Journal of Medicinal Chemistry 2009;59:4306–18.
[18] Pandey SK, Sajjad M, Chen Y, Zheng X, Yao R, Missert JR, et al. Comparative positron-emission tomography (PET) imaging and phototherapeutic potential of ^{124}I-labeled methyl- 3-(1′-iodobenzyloxyethyl)pyropheophorbide-a vs the corresponding glucose and galactose conjugates. Journal of Medicinal Chemistry 2009;52:445–55.
[19] Perrin DD, Armarego WLF. Purification of laboratory lhemicals. England: Pergamon Press; 1988.
[20] Lange SJ, Nie H, Stern CL, Barrett AGM, Hoffman BM. Peripheral palladium(II) and platinum(II) complexes of bis(dimethylamino)porphyrazine. Inorganic Chemistry 1998;37:6435–43.
[21] Forsyth TP, Williams DBG, Montalban AG, Stern CL, Barrett AGM, Hoffman BM. A facile and regioselective synthesis of trans-heterofunctionalized porphyrazine derivatives. Journal of Organic Chemistry 1998;63:331–6.
[22] Wöhrle D, Eskes M, Shigehara K, Yamada A. A simple synthesis of 4,5-disubstituted 1,2-dicyanobenzenes and 2,3,9,10,16,17,23,24-octasubstituted phthalocyanines. Synthesis; 1993:194–6.
[23] Greene TW, Wuts PGM. Protective groups in organic synthesis. New York: John Wiley and Sons, Incorporation; 1999.

[24] Dziadek S, Brocke C, Kunz H. Biomimetic synthesis of the tumor-associated (2,3)-sialyl-T antigen and its incorporation into glycopeptide antigens from the mucins MUC1 and MUC4. Chemistry-A European Journal 2004;10:4150–62.
[25] Sibert JW, Bauman TF, Williams DJ, White AJP, Barrett AGM, Hoffman BM. Gemini-porphyrazines: the synthesis and characterization of metal-capped cis- and trans-rorphyrazine tetrathiolates. Journal of the American Chemical Society 1996;118:10487–93.
[26] De la Tore G, Martínez-Diaz MV, Ashton PR, Torres T. Novel homo- and heterodimetallic heterobinuclear phthalocyaninato-triazolehemiporphyrazinate complexes. Journal of Organic Chemistry 1998;63:8888–93.
[27] Gouterman M. Optical spectra and electronic structure of porphyrins and related rings. The porphyrins. New York: Academic Press; 1978.
[28] Mack J, Kirby S, Ough EA, Stillman MJ. Ground-state and optical spectrum of metallophthalocyanine radical anions from low-temperature magnetic circular dichroism spectroscopy. Inorganic Chemistry 1992;31:1717–9.
[29] Corey MG, Hirose H, Zerner MC. Calculated structures and electronic absorption spectroscopy for magnesium phthalocyanine and its anion radical. Inorganic Chemistry 1995;34:2969–79.
[30] Stuzhin PA, Bauer EM, Ercolani C. Syntheses and properties of tetrakis(thiadiazole) porphyrazine and its magnesium and copper derivatives. Inorganic Chemistry 1998;37:1533–9.